THE PENNSYLVANIA STATE UNIVERSITY
SCHREYER HONORS COLLEGE

DEPARTMENT OF PHYSICS

FRUSTRATED MAGNETISM IN OUT-OF-PLANE AND IN-PLANE SYSTEMS

CHRIS GRIGAS
SUMMER 2013

A thesis
submitted in partial fulfillment
of the requirements
for baccalaureate degrees
in Physics and Mathematics
with honors in Physics

Reviewed and approved* by the following:

Peter Schiffer
Professor of Physics
Co-Thesis Supervisor

Jorge Sofo
Professor of Physics
Co-Thesis Supervisor

Richard Robinett
Professor of Physics
Honors Advisor

* Signatures are on file in the Schreyer Honors College.

ABSTRACT

This thesis presents work related to the study of systems of frustrated nanomagnet arrays, or artificial spin ice, whose moments are oriented perpendicularly from the plane of the sample. It builds off of previous work by the same research group that has been done studying various other geometries of frustrated nanomagnet arrays.

Frustration is a phenomenon found in real 3D materials like holmium stanate and holmium titanate which are called spin ices. Artificial spin ice is a useful model system for studying the behavior of these materials and provides several advantages over the real materials. Advanced lithographic techniques allow the specific interactions between the islands to be finely tuned and the length scale of the samples is such that they can be relatively easily imaged by techniques such as atomic force microscopy and magnetic force microscopy (AFM/MFM).

This thesis explores the work that has been done on various lattice geometries with a particular emphasis on lattices whose constituent islands have their moments oriented perpendicularly to the plane of the sample. There are many parts to studying these materials; design of the islands, fabrication, demagnetization, and imaging. Of these steps this thesis places a particular emphasis on the techniques that are used to image the samples and extract meaningful data from them.

Correlations in the orientation of islands in perpendicularly magnetized arrays, in kagome and honeycomb lattices, were computed for island pairs of differing distances. It is seen that the correlations between nearest-neighbor pairs of islands are strongest and then decay dramatically for higher order island pairs. Fitting this data to two different simulations

shows that the correlations in perpendicularly magnetized arrays are dominated by nearest-neighbor interactions and, by analogy, the same conclusion holds for in-plane hexagonal arrays. The similarities between two very different realizations of spin ice suggest that the behavior of spin ice is independent of the particular geometry and material of the lattice, which could be further explored by studying different geometries.

Demonstration of lattices with perpendicularly oriented moments opens up possibilities of using artificial spin ices to imprint a magnetic topology onto a thin film. This could have applications in diverse fields ranging from 2D electron gases to superconductors.

TABLE OF CONTENTS

LIST OF FIGURES

ACKNOWLEDGEMENTS

I would like to acknowledge the support of both Prof. Richard Robinett, my undergraduate advisor, whose advice has been invaluable throughout my undergraduate career and Prof. Peter Schiffer, my co-thesis advisor, for giving me the opportunity to work for him and to develop my research knowledge. I would also like to extend a special thanks to Prof. Jorge Sofo, my other co-thesis advisor, who graciously volunteered his time to assist me in completing this thesis. I would also like to thank my graduate student research mentors who taught me the basics of doing research: Jie Li, Sheng Zhang, and Ian Gilbert. Without them I never would have been able to learn all that I did.

I would also like to thank my family and friends, especially those in the Society of Physics Students, who helped me to get through the tough times.

Introduction

Frustration

It is basic physics that any system will try to find its lowest energy configuration, but what happens if there is some reason that a system cannot access its lowest energy configuration? This phenomenon is called ‘frustration’ and it occurs when the constituent pieces of a system compete in such a way that not all of the elements can reach their minimum energy configuration [1].

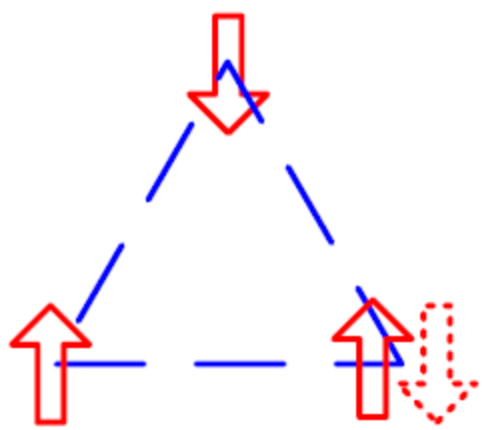

Figure 1: The simplest possible frustrated geometry is an equilateral triangle with spins placed on the three corners of the triangle. Not all of the pairwise interactions between the spins can be minimized at the same time. Figure from [2].

One way that frustration can emerge is because of the geometry of a lattice. This kind of frustration is called geometrical frustration. Geometrical frustration arises when competing interactions forbid all lattice site interactions from being minimized simultaneously. These competing interactions can be atomic bonding, as in water ice [3], spin-spin interactions [4], as in spin ice materials, or dipolar exchange interactions [5].

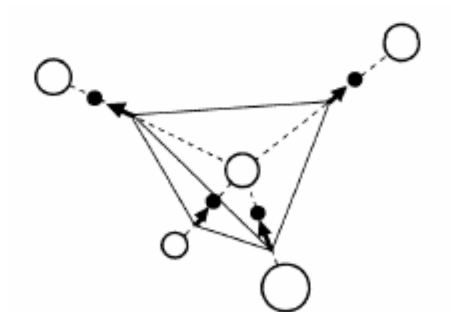

Figure 2: A single tetrahedra unit cell of the water ice lattice. The oxygen atom is located at the center of the tetrahedra and is surrounded by four protons. Two of these protons are closer to the central oxygen atom and two of the protons are farther away from oxygen atom.. This is the 'two-in, two-out' ice rule. Figure from [6].

The simplest example of frustration is placing three antiferromagnetic spins on the corners of an equilateral triangle, as illustrated in Figure 1. Not all of the pairwise interactions between these three spins can minimized at once. In fact there is a 6-fold degeneracy in the ground state of this system. This simple system can be repeated in various ways to create extended frustrated lattices.

The classic example of frustration in nature is water ice. Water ice forms a lattice of corner sharing tetrahedra, called a pyrochlore lattice, with the oxygen atoms sitting in the middle of the tetrahedra and the protons sit on lines between all of the oxygen atoms. These

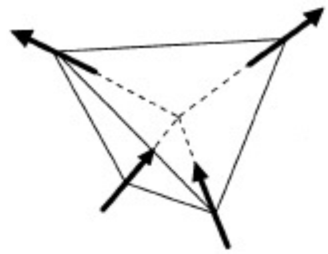

Figure 3: The 'two-in,two-out' ground state configuration of the magnetic spins in spin ice materials. Figure from [7].

protons are not an equal distance from all of the oxygen atoms. Two of the protons will be closer to the oxygen atom and two of them will be farther away, as shown in Figure 2. This is commonly referred to as the ‘2-in,2-out’ ice rule. This arrangement has a 6-fold ground state degeneracy [3].

There is also another class of materials that mimic much of the behavior of water ice except they exchange the atomic interactions of water ice for spin-spin interactions. Appropriately these materials are called ‘spin ices’ (Figure 3). These materials are all rare earth pyrochlores, two examples of which are holmium titanate ($Ho_2Ti_2O_7$) [7] and dysprosium titanate ($Di_2Ti_2O_7$) [8]. These materials also have a corner sharing tetrahedral lattice with the magnetic ions sitting at the corners of the tetrahedra. The magnetic moments of the ions are forced to either point directly towards or directly away from the center of the tetrahedra, essentially making them large Ising spins. In the ground state two of the spins point in towards the center of the tetrahedra and two of the spins point outwards, a behavior analogous to the ‘two-in,two-out’ ice rule [7]. This leads to these materials being called ‘spin ices’.

Artificial Spin Ice

There are several difficulties in trying to study frustrated spin ices. Frustration is highly dependent on the geometry of the lattice and the specific interactions in the material, which both cannot be tuned with current technology. Defects in the lattice, which are inevitable, also complicate the process of understanding frustration. Finally, current technology is incapable of imaging individual spins and therefore we cannot know how they accommodate the frustration.

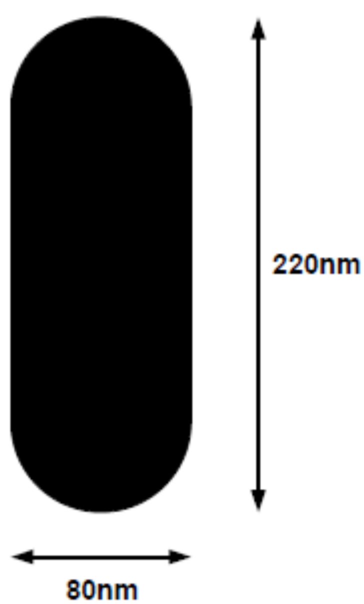

Figure 4: The design of the permalloy islands. Figure from [2].

One way to circumvent all of these issues is to create a model system that can display similar behavior, but on a much larger length scale so that the individual moments can be imaged. To this end large lattices of lithographically fabricated nanomagnets were fabricated out of an antiferromagnetic material called permalloy, $Ni_{0.81}Fe_{0.19}$. Given the proper dimensions, shown in Figure 4, the islands can be single domain and the magnetic moment can be forced to point along the long axis of the island.

A software package called OOMMF (object oriented micromagnetic framework) which does micromagnetic simulations was used to design the islands. The island design that

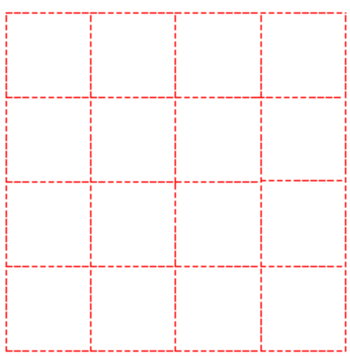

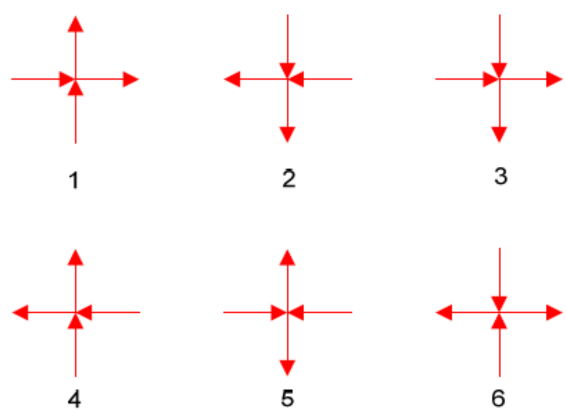

Figure 5: (left) Projecting a 3D pyrochlore lattice onto its (110) produces a two dimensional square lattice that can serve as a model of the real system. (right) This model must also follow the 'two-in,two-out' ice rule which limits the number of accesible ground state configurations to 6, down from the total of 16 possible configurations. Figure from [2].

was settled on was shaped like a rectangle with half-circles on either end. It has a length of 220 nm and a width of 80 nm. From the simulations it was found that this shape paired a strong shape anisotropy, which forces the magnetic moment to point along the long axis, with a single domain remnant state as well as Ising-like switching between states. These properties make it most similar to an Ising spin.

A Two-Dimensional Model for Frustration

Projecting a pyrochlore crystal onto a two dimensional plane going through (110) produces a square lattice of points (or vertices) connected by edges to each other [11]. In this two dimensional model the magnetic spins can point right or left and up or down giving a total of 16 possible configurations of any given vertex. Analogously to the real 3D frustrated materials this model also must obey the ‘two-in, two-out’ ground state configuration. This drastically reduces the number of possible configurations from 16 down to only 6. This procedure is illustrated in Figure 5.

Demagnetization and Imaging Procedure

Demagnetization

Before the fabricated arrays can be measured they need to have a zero net magnetic moment. In order to do this the arrays are initially placed in a magnetic field greater than 770 Oe [11], which is the coercive field of the islands. The arrays are then rotated at 1000 rpm [13] in the field while it is reduced in steps of 1.6 Oe [14]. At each step down in field the field is also reversed in direction. This procedure was found to be the most effective at demagnetizing the arrays.

MFM/AFM Imaging

The arrays can be imaged once they have demagnetized. They are imaged using a Veeco combination atomic and magnetic force microscope (AFM/MFM). An AFM/MFM can operate in two modes, static and dynamic [15]. The dynamic mode is typically preferred over the static mode as it is more sensitive. The first pass over the array is done using the atomic force microscope; This process scans an atomically sharp tip over the sample and measures the force acting on the tip. This allows the machine to map the topology of the sample. After this process is complete the machine makes a second pass over the sample using the MFM which will detect the arrangement of the magnetic moments in the islands. In the dynamic mode, an MFM (AFM) functions by scanning a magnetic (atomically sharp) tip on the end of a cantilever over the sample. The cantilever is oscillated at a known frequency which is measured by a laser beam that is reflected off of the top of the cantilever. The interaction between the tip and the sample will produce a phase shift in the oscillation of the cantilever and this can be measured and used to calculate the force that the sample is exerting on the tip. The magnitude and direction of this force is then displayed over the topographic image that the AFM produced and used to display the magnitude and direction of the domain.

In order to calculate this force the cantilever is assumed to be a simple harmonic oscillator with an applied force given by $F_z = F_0 \cos(\omega t)$ and the resulting displacement given by $z = z_0 \cos(\omega t + \phi)$. The amplitude and phase shift of the resulting motion are given by equation (1).

$$z_0 = \frac{\frac{F_0}{m}}{\sqrt{(\omega_n^2 - \omega^2) + (\frac{\omega_n \omega}{Q})^2}}, \ \varphi = tan^{-1}\left(\frac{\omega_n \omega}{Q(\omega_n^2 - \omega^2)}\right) \qquad (1)$$

where $\omega_n = \sqrt{(k/m)}$ is the natural frequency of the oscillator, $Q = 1/2\delta$ is the quality factor, and $\delta = D/(2\sqrt{(mk)})$ is the damping factor. The forces acting on the magnetic tip act to change the spring constant of the simple harmonic oscillator which produces a change in the resonant frequency of the cantilever. Therefore the resonant frequency is given by equation (2).

$$\omega_r = \omega_n \sqrt{1 - \frac{1}{k}\frac{\partial F_z}{\partial z}} \qquad (2)$$

where ω_n is the natural resonant frequency of the oscillator and ω_r is the new resonant frequency due to the interaction with the sample. The changes in the resonant frequency will be small, therefore we can take the Taylor expansion of the radical in this equation and keep only the first term.

$$\omega_r \approx \omega_n \left(1 - \frac{1}{k}\frac{\partial F_z}{\partial z}\right) \qquad (3)$$

Taking the difference between the natural resonant frequency and the modified resonant frequency gives equation three.

$$\Delta f = f_r - f_n \approx \frac{-f_n}{2k}\frac{\partial F_z}{\partial z} \qquad (4)$$

where $f = \omega / 2\pi$. Here the force gradient ∇F can be solved for and its magnitude and direction can be plotted on the image.

Image Analysis

Overview

When the AFM/MFM image capturing process is complete the image typically resembles that given in Figure 6. While it would be fairly easy to go through and manual determine the orientation of the moments in this particular image it is a very tedious process, and if the lattices have a much shorter lattice constant it can be very difficult for a human to determine the orientation of the moments without losing track of their position in the lattice. This makes manually analyzing the image both a tedious and inaccurate prospect. In order to alleviate this problem, code was written in MATLAB [16] that can help the image analyzer to accurately and quickly process an image.

There are five distinct steps in processing an image produced by the MFM. First, the image is imported to MATLAB and converted to grayscale. Second, the user defines the borders of the lattice for the code and inputs the number of rows and columns in the lattice into the program. Then the program iterates through the image and compares each unit cell in the array with an ideal image to determine the arrangement of the moments in that cell. Once all of these moment configurations are determined the program plots them in an image and then compares the produced image with the original image in order to check for errors.

Importing and Converting the Image

The first step in the image analysis process is to import the image produced by the MFM into MATLAB. The MFM saves the images in RGB format, but the analysis is concerned only with the intensity of light coming from the image, so the imported images must be converted to grayscale before they are useful. There are several different methods for converting an RGB image to grayscale but the method used here is called the 'luminosity' method [17]. The luminosity method takes a weighted average of the three color components

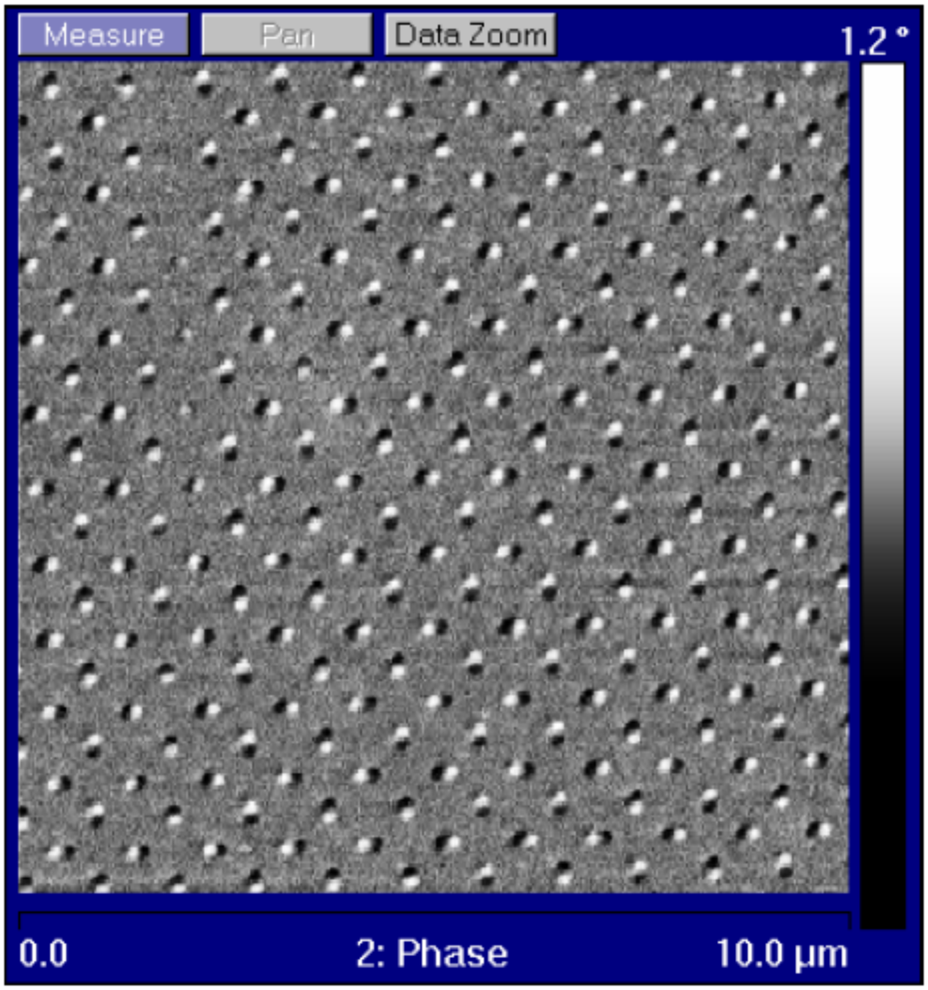

Figure 6: An example of what an image produced by the MFM which images the arrays looks like. Determining the orientation of the moments of each of the islands is the primary goal of the image analysis process. Figure from [2].

(red, green, and blue) but it varies the weights on each based upon how brightly human eyes perceive each color. Therefore the luminance L is calculated as in equation 5.

$$L = 0.2989\mathrm{R} + 0.5870\mathrm{G} + 0.1148\mathrm{B} \tag{5}$$

Human eyes perceive green as brighter than red and blue, therefore the weight on the green component of the RGB image is much greater than the other. This produces a grayscale image that looks much more like the original RGB image to human eyes.

Defining the Parameters of the Image

The MFM produces images that look similar to Figure 6. Obviously the blue border around the image is not useful information so the user has to define the four corners of the image to the program. The user does this by specifying the coordinates of the vertices in the

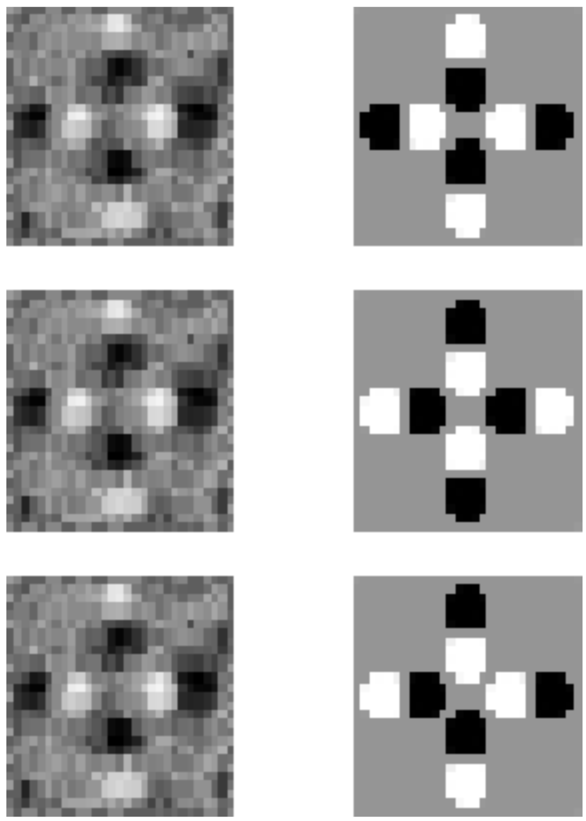

Figure 7: Comparing the images of a real vertex (left column) with the ideal images (right column). The inner product of the two images in the first row would be much greater than zero while the inner product of the two images in the second row would be much less than zero. The third row would have an inner product approximately equal to zero.

four corners of the image. All four corners need to be specified because there can be a significant amount of slant to the image. The user then counts the number of rows and columns of unit cells. The program uses this information to define the size of a unit cell in pixels.

Determining the Moment Orientations

The orientations of the moments in a specific vertex are determined by convolving the matrix of the real image with an ideal matrix. Convolution here is simply taking an inner product between the two matrices. The output of this operation determines if the real matrix matches the ideal matrix. There are three possible outcomes of the convolution of the two matrices.

1) The product of convolution of the two matrices is roughly zero. (the third row in figure 7)
2) The product of the convolution of the two matrices is greater than or equal to some threshold value. (the first row in figure 7)
3) The product of the convolution of the two matrices is less than or equal to the negative of the threshold value. (the second row in figure 7)

In the first case, the product is roughly zero, the orientation of the moments in the real image are determined to not match the ideal image. Due to noise in the image there may be some correlation between the ideal image and the real image that is being tested. To combat this a ‘threshold’ value is set. In the second case, where the product of the two matrices is greater than or equal to the threshold value, the matrix being tested is determined to have the same moment configuration as the ideal matrix it is being tested against. In the third case, where the product of the two matrices is less than or equal to the negative of the threshold value, the matrix being tested is determined to have the exact opposite moment configuration as the matrix it is being tested against.

Each vertex in the array will be tested against the ideal vertices until one is found whose convolution with the real vertex is greater than the set threshold value. The third case from above means that the real image will only have to be tested against a maximum of eight different vertices before a match is found. When a match is found the orientations of the moment will be input into a spreadsheet as either positive or negative one.

Setting the threshold at an appropriate value is an important part of this process. In an image that is not very noisy the threshold should be set at a very low level. The lack of noise will prevent the product of unlike vertices from exceeding the threshold and giving a false reading. Therefore the threshold needs to be set at a low level to ensure that all of the vertices that are alike exceed the threshold value. If the image is very noisy then it becomes more likely that taking the convolution between two unlike vertices will exceed the threshold if it is not set high, but if it is set too high then there is the risk that the product of like vertices will not result in a high enough value. Figuring out exactly how high or how low to set the

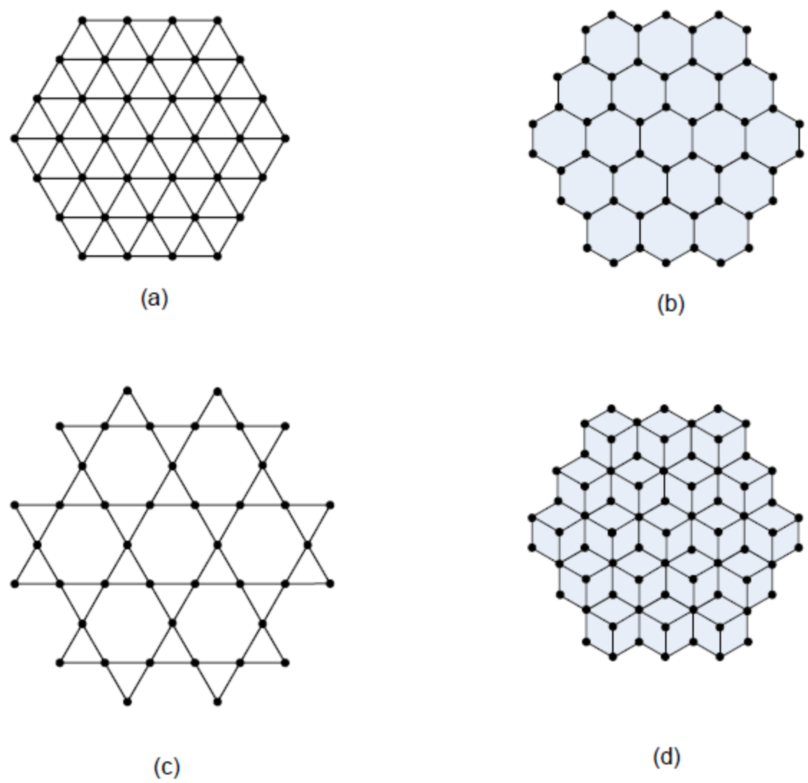

Figure 8: Examples of some of the classic frustrated lattice geometries. (a) triangular, (b) hexagonal (honeycomb), (c) kagome, and (d) centered hexagonal. Figure from [18].

threshold value is simply a matter of trial and error before an intuitive sense for setting the value develops.

Error Checking

The final step in the process of analyzing the image is to check to make sure that the program has accurately determined the moment orientations. To do this the program creates another image by superimposing the created image over top of the original image. In this image an island is black if the program has assigned it the correct orientation, and an island is white if the program has assigned it the incorrect orientation. It is then up to the user to manually determine the correct orientation of that island.

Lattice Geometries of Interest

There are many different lattice geometries that have been investigated in this experiment. These lattices include ones whose islands interact in the plane with the other islands and those whose moments are directed perpendicularly from the surface of the lattice. The in-plane lattices that have be examined are the square, hexagonal, and triangular lattices. The perpendicular lattices that were examined were the hexagonal and kagome lattices. Examples of some of these lattices are given in Figure 8 above.

Perpendicular Magnetization

Fabrication

The discussion in this paper so far has been confined to talking about islands whose moments point in the plane of the lattice, but it is also possible to have frustration in a system where the magnetic moments are directed out of the plane.

These islands were fabricated with multiple layers of thin metallic films with the structure Ti(20 Å)/Pt(100 Å)/[Co(3 Å)/Pt(10 Å)]$_8$ deposited by electron-beam evaporation after electron-beam patterning of a bi-layer resist. The arrays are then demagnetized by following a similar procedure as the one outlined above. The samples are first placed in a field of 2000 Oe to coerce all of the moments into pointing in the same direction. They were then rotated at 1000 rpm while the field was stepped down in increments of 1.6 Oe and the direction was reversed at each step. After the samples were demagnetized they were then imaged with an MFM [19].

Analysis

Adapting the previously written code to analyze these images, and then analyzing those images, was one of the main goals of this thesis. The code functions in much the same way as it does for the in-plane geometries with some slight differences. First, the perpendicular islands have a different geometry than the in-plane islands so a new model image had to be used. The perpendicular island code also had to be modified to use a slightly different model vertex to analyze the image. In the in-plane geometries the islands are

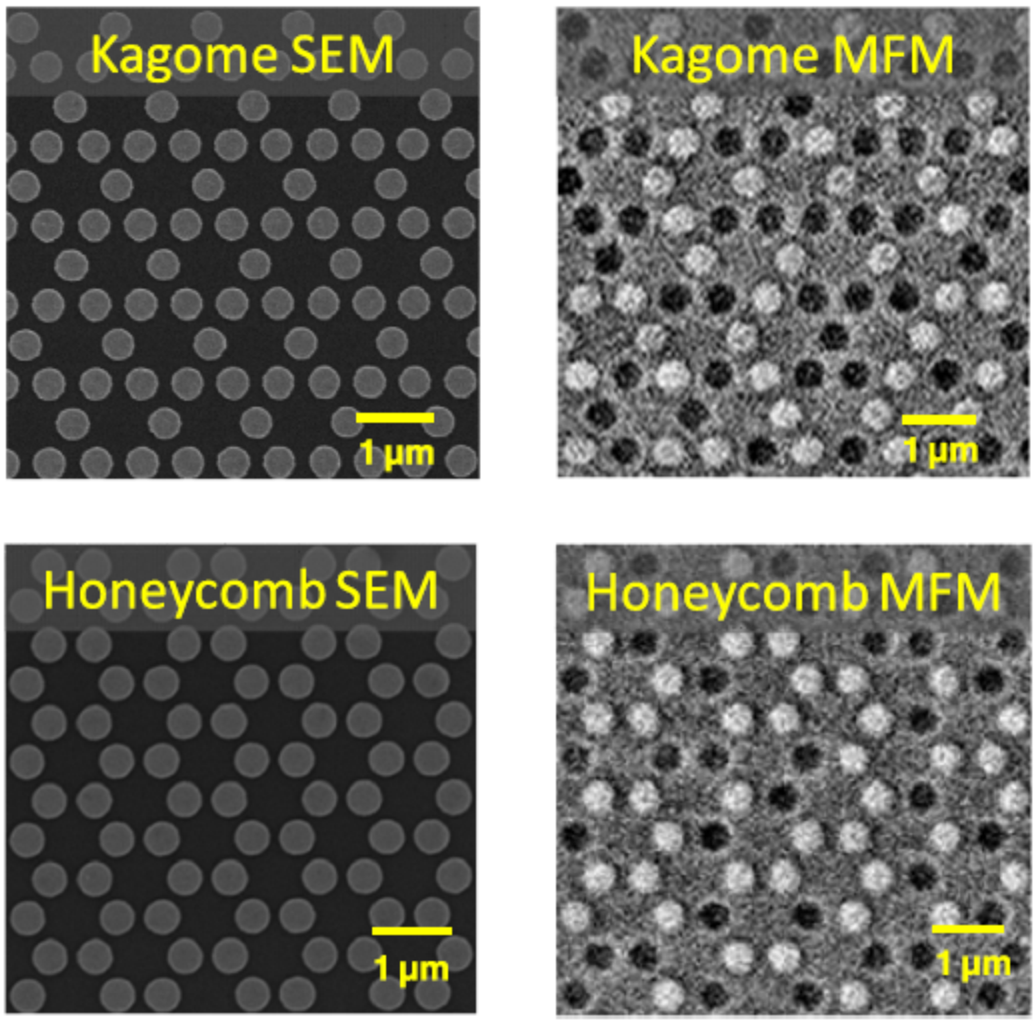

Figure 9: SEM (left column) and MFM (right column) images of the two perpendicular moment geometries. These two geometries are the kagome (top row) and honeycomb lattices (bottom row). Figure from [19].

stadium shapes and they occupy the edges of the shapes that make up the lattice. In the out-of-plane samples the islands are circles that sit on the vertices of the lattice, so the code needed to adjusted to deal with this.

These lattices were studied by considering the pairwise correlations of the orientations of the moments, where the pairwise correlations were defined as the average spin product over all island pairs of a specific order (see Figure 10 for pair orders). Parallel aligned moments were defined to be a +1 and antiparallel aligned moments were defined to be a -1. These correlations were calculated for pairs of islands of various orders. The nearest neighbors to an island are defined to be the first order islands, next nearest neighbors are the second order islands, etc. These correlations were studied for three different geometries; the perpendicular kagome, perpendicular honeycomb, and the in-plane hexagonal. The perpendicular kagome and perpendicular honeycomb are diagrammed in Figure 10 (d and e) and the in-plane hexagonal lattice is diagrammed in Figure 8(b). The correlations are strongest at the shortest lattice constant in this experiment, 500 nm, and decrease drastically at larger lattice constants. Therefore the data from smallest lattice constant arrays are shown here. For each of the geometries the absolute correlations between the nearest neighbor islands are greatest and then they decrease monotonically towards zero.

Simulation

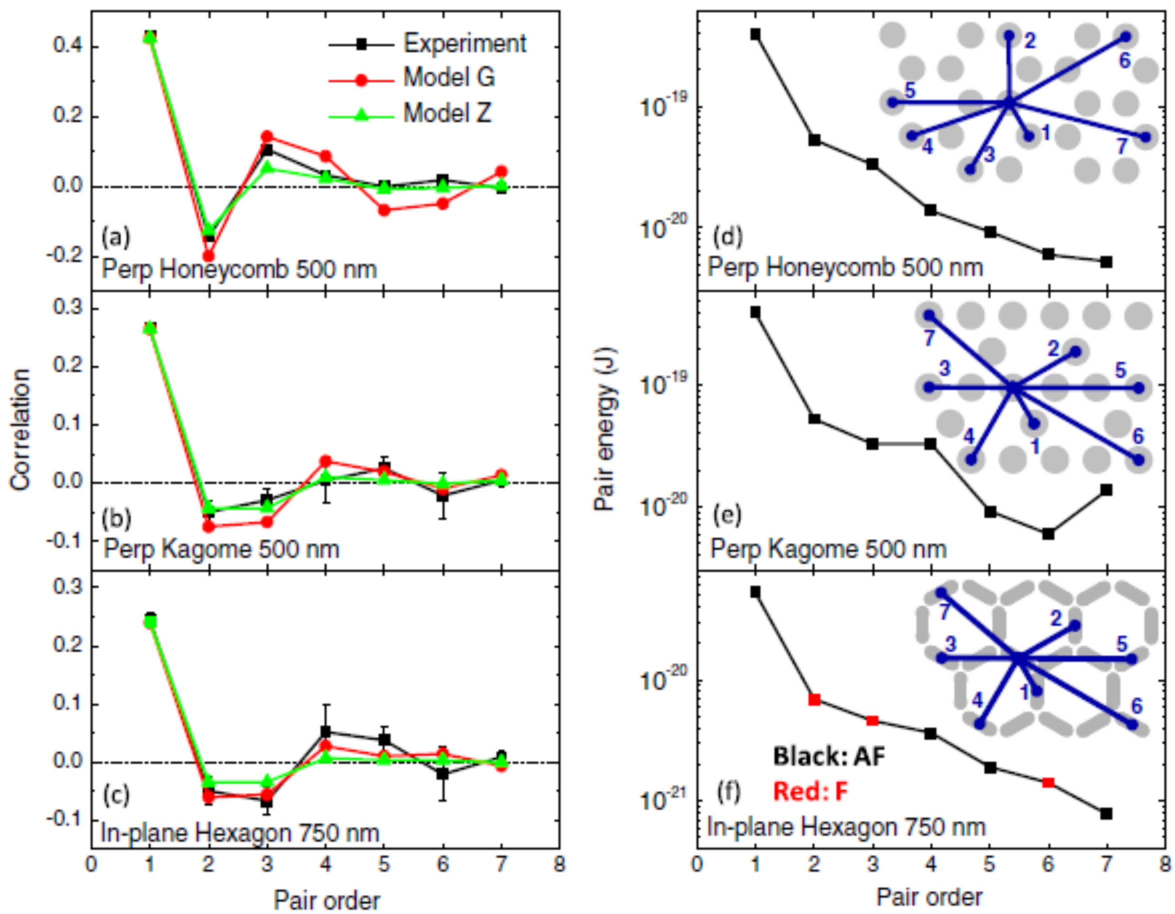

Figure 10: (a),(b), (c) The correlations between the orientations of the islands are strongest for nearest-neighbor pairs of islands and they decrease monotonically, in absolute value, to zero. All three geometries show a strikingly similar behavior in spite of having different geometries and composition. Figure from [19].

Two simulations were done in order to better understand the behavior of the system. One was a quasiequilibrium Gibbsian model (called model G) and the other was a kinetic zero-temperature quenched model (called model Z). Model G defined a nearest-neighbor interaction function as in equation 6.

(6)

$$\Phi(s) = \sum_{NN\,Pairs} s_i s_j$$

Then probability of any given configuration of the system is $e^{(\Phi(s))}$ .The overall state is then calculated using standard Monte Carlo methods [20]. Model Z starts with a random configuration of the moments in the lattice and then selects individual moments out of that lattice. The simulation will then flip the orientation of that selected moment if doing so will reduce the nearest-neighbor interaction energy. It then proceeds in this manner until the nearest-neighbor correlation value matches that of the experiment.

Conclusion

Both of these models accurately reproduce the experimental results, as figure 10 shows. The fact that two very different models accurately reproduce the experimental results suggests that the equilibrium state of the system is controlled only by the topology of the lattice and the correlation between nearest-neighbor islands. If it is the case that nearest-neighbor interactions dominate then an ordered ground state would be expected in the honeycomb lattice. Indeed, as Figure 11 shows, we do observed domains in the honeycomb lattices.

As Figure 10 (b) and (c) show, there is a clear similarity between the moment correlations of the perpendicular kagome and the in-plane hexagonal arrays. The natural question to ask after this observation is how that similarity would evolve with changing interaction energy between the nearest-neighbor islands, which can be changed by changing the lattice constant. Figure 12 plots the nearest neighbor correlations against the nearest neighbor interaction energies.

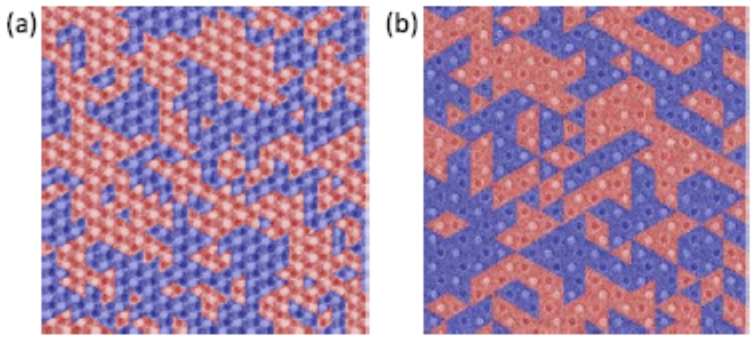

Figure 11: Domains in honeycomb lattices with lattice constants of (left) 500 nm and right (800) nm. Figure from [19].

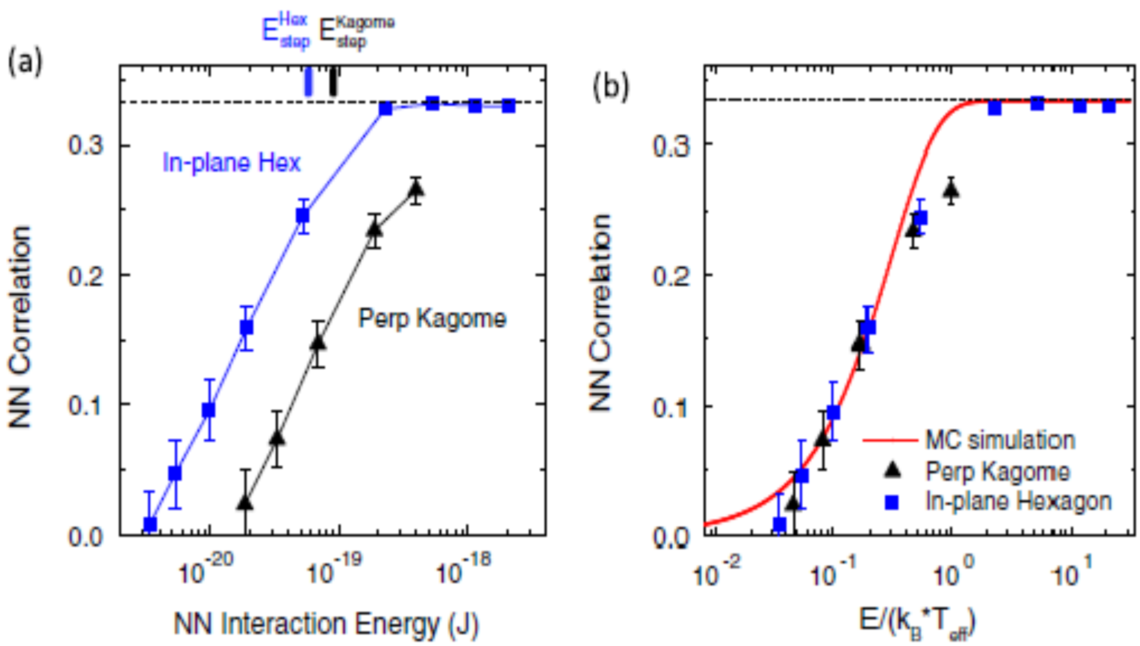

Figure 12: (left) Nearest-neighbor correlations plotted against interaction energy for all of the inter-island spacings. (right) Nearest-neighbor correlations plotted against the interaction energy scaled by the effective temperature to match the data from a monte carlo simulation of an ideal ising kagome antiferromagnet. Figure from [19].

In order to model the data a Monte Carlo simulation of an ideal nearest-neighbor Ising kagome antiferromagnet which had been thermalized at an effective temperature, T_{eff} , was performed. The solid line in Figure 12 (b) represents the result of this simulation scaled by the effective temperature. T_{eff} is taken to be $3.3\,x\,10^5 K$ for perpendicular kagome and $7.9\,x\,10^4 K$ for the in-plane hexagonal array. This simulation technique captures most of the behavior of the experimental data. The only part that it misses is the way in which the correlation goes to zero. The simulation shows a slow, asymptotic approach to zero whereas the data has a threshold transition from an uncorrelated to a correlated state.

The striking similarities between the correlation data for all three geometries (Figure 10) suggest that the behavior of artificial spin ices does not depend on the particular geometry or the make up of the islands. The natural extension of this would be to take similar data for a different set of geometries. Demonstrating that lattices with perpendicularly oriented moments can be constructed open up the door for using these lattices to imprint a frustrated magnetic topology onto a thin film. This procedure could have implications in diverse fields such as 2D electron gases and superconductors.

BIBLIOGRAPHY

1. A. P Ramirez, Ann. Rev. Mater. Sci. 24, 453 (1994)

2.Wang, Ruifang. Doctoral Thesis. “Geometrical Magnetic Frustrations and Demagnetization of Artificial Spin Ice” (2007).

3. L. C. Pauling, J. Am.Chem.Soc. **57**, 2680 (1935).

4. A. P. Ramirez, Ann. Rev. Mater. Sci. **24**, 453 (1994).

5. R. Moessner, Can. J. Phys **79**, 1283 (2001).

6. J. Snyder, J. S. Slusky, R. J. Cava, and P. Schiffer, Nature **413**, 48 (2001).

7. Harris, M. J., Bramwell, S. T., McMorrow, D. F., Zeiske, T., & Godfrey, K. W. Phys. Rev. Lett.*,* **79** (13), 2554-2557. (1997)

8. M. J. Harris, S. T. Bramwell, D. F. McMorrow, T. Zeiske, and K. W. Godfrey, Phys. Rev. Lett. **79**, 2554 (1997).

9. Ramirez, A. P., Hayashi, A., Cava, R. J., Siddharthan, R., & Shastry, B. S. Nature*,* **399** (6734), 333-335. (1999).

10. M. J. Harris, S. T. Bramwell, D. F. McMorrow, T. Zeiske, and K. W. Godfrey, Phys. Rev. Lett. **79**, 2554 (1997).

11. E. H. Lieb and F. Y. Wu, “Phase transition and critical phenomena” **vol. 1**, 1972. Academic Press.

12. Wang, R. F., Li, J., McConville, W., Nisoli, C., Ke, X., Freeland, J. W., et al. Journal of Applied Physics, **101** (9), 09J104. (2007).

13. Wang, R. F., Nisoli, C., Freitas, R. S., Li, J., McConville, W., Cooley, B. J., et al. Nature, **439** (7074), 303-306. (2006).

14. Li, J., Zhang, S., Bartell, J., Nisoli, C., Ke, X., Lammert, P. E., et al. Physical Review B, **82** (13), 134407. (2010).

15. Qi, Y., Brintlinger, T., & Cumings, J. Physical Review B, **77** (9), (2008).

16. McConville, William F. (Penn State honors thesis). (2007)

17. Cook, John D. Online: http://www.johndcook.com/blog/2009/08/24/algorithms-convert-color-grayscale/ (2009)

18. R. Liebmann "Statistical Mechanics of Periodic Frustrated Ising Systems" Springer-Verlag, Berlin Heidelberg, (1986).

19. Zhang, Sheng et al. Phys. Rev. Lett. **109**. 087201. (2012).

20. P. E. Lammert, X. L. Ke, J. Li, C. Nisoli, D. M. Garand, V. H. Crespi, and P. Schiffer, Nature Phys. 6, 786 (2010).

Chris Grigas

115 James St
Leola, PA 17540
Cell: (717) 283-5269
Email: cjg5210@psu.edu

Objective

- To obtain a job that allows me to apply my technical/analytical skills and mathematical modeling skills to challenging and interesting problems for the benefit of my employer

Qualifications:

- Analytical personality
- Excellent problem solving skills
- Loves to learn new subjects
- Leadership and organizational skills

Education

- Penn State University -- May 2013
  - B.S. in Physics
  - B.S. in Mathematics
- Conestoga Valley High School – June 2009

Employment

- Lab of Professor Peter Schiffer – 2010 - 2012
  - Responsible for image processing and analysis of data taken
- Kevin Stoltzfus Hardwood Flooring – Summer 2009
  - Installation, finishing, and refinishing of hard wood floors

Internships

- Baylor University
  - National Science Foundation – Research Experience for Undergraduates summer fellow 2012
- Penn State University
  - National Science Foundation – Research Experience for Undergraduates summer fellow 2011

Honors

- Member of the Schreyer Honors College
- Dean's list – All semesters
- Member of Sigma Pi Sigma
  - Physics honor society

Extracurricular

- Society of Physics Students
  - President – 2012
  - Physics outreach and education, professional development